

LETTERS

Regulation of inflammatory responses by gut microbiota and chemoattractant receptor GPR43

Kendle M. Maslowski^{1,2,3}, Angelica T. Vieira^{1,4}, Aylwin Ng⁵, Jan Kranich^{1,2}, Frederic Siero¹, Di Yu¹, Heidi C. Schilter^{1,2,3}, Michael S. Rolph^{1,2}, Fabienne Mackay^{1,6}, David Artis⁷, Ramnik J. Xavier^{5,8}, Mauro M. Teixeira⁴ & Charles R. Mackay^{1,2,3,6}

The immune system responds to pathogens by a variety of pattern recognition molecules such as the Toll-like receptors (TLRs), which promote recognition of dangerous foreign pathogens. However, recent evidence indicates that normal intestinal microbiota might also positively influence immune responses, and protect against the development of inflammatory diseases^{1,2}. One of these elements may be short-chain fatty acids (SCFAs), which are produced by fermentation of dietary fibre by intestinal microbiota. A feature of human ulcerative colitis and other colitic diseases is a change in 'healthy' microbiota such as *Bifidobacterium* and *Bacteriodes*³, and a concurrent reduction in SCFAs⁴. Moreover, increased intake of fermentable dietary fibre, or SCFAs, seems to be clinically beneficial in the treatment of colitis^{5–9}. SCFAs bind the G-protein-coupled receptor 43 (GPR43, also known as FFAR2)^{10,11}, and here we show that SCFA–GPR43 interactions profoundly affect inflammatory responses. Stimulation of GPR43 by SCFAs was necessary for the normal resolution of certain inflammatory responses, because GPR43-deficient (*Gpr43*^{−/−}) mice showed exacerbated or unresolving inflammation in models of colitis, arthritis and asthma. This seemed to relate to increased production of inflammatory mediators by *Gpr43*^{−/−} immune cells, and increased immune cell recruitment. Germ-free mice, which are devoid of bacteria and express little or no SCFAs, showed a similar dysregulation of certain inflammatory responses. GPR43 binding of SCFAs potentially provides a molecular link between diet, gastrointestinal bacterial metabolism, and immune and inflammatory responses.

Recent evidence suggests that products of intestinal microbiota might positively influence inflammatory disease pathogenesis^{1,2}. To identify factors produced by bacteria that might be beneficial to host immune responses, we induced colitis chemically by adding dextran sulphate sodium (DSS) to the drinking water of germ-free mice. The absence of bacteria from these mice, and the consequences this had on immune responses, resulted in significantly worse colonic inflammation, compared to conventionally raised (CNV) mice. Germ-free mice treated with DSS had decreased weight, an increased daily activity index (DAI; a combined measure of weight loss, rectal bleeding and stool consistency) and a decreased haematocrit (Fig. 1a). Germ-free mice re-colonized with gut microbiota, by gavaging with CNV faeces, showed a marked reduction in inflammation (Supplementary Fig. 1), indicating that the exacerbated response related to lack of bacterial colonisation of the gut. Products of bacteria that have been reported to show anti-inflammatory properties include SCFAs, which are produced by colonic bacteria after fermentation of dietary fibre. Bacteria of the *Bacteroidetes* phylum produce high levels of acetate and propionate, whereas bacteria of the

Firmicutes phylum produce high amounts of butyrate¹². Germ-free mice do not produce SCFAs owing to a lack of enteric microbes¹³. Treatment of germ-free mice with 150 mM acetate in the drinking water markedly improved disease indices, with an increase in colon length, decreased DAI and levels of the inflammatory mediator myeloperoxidase (MPO)

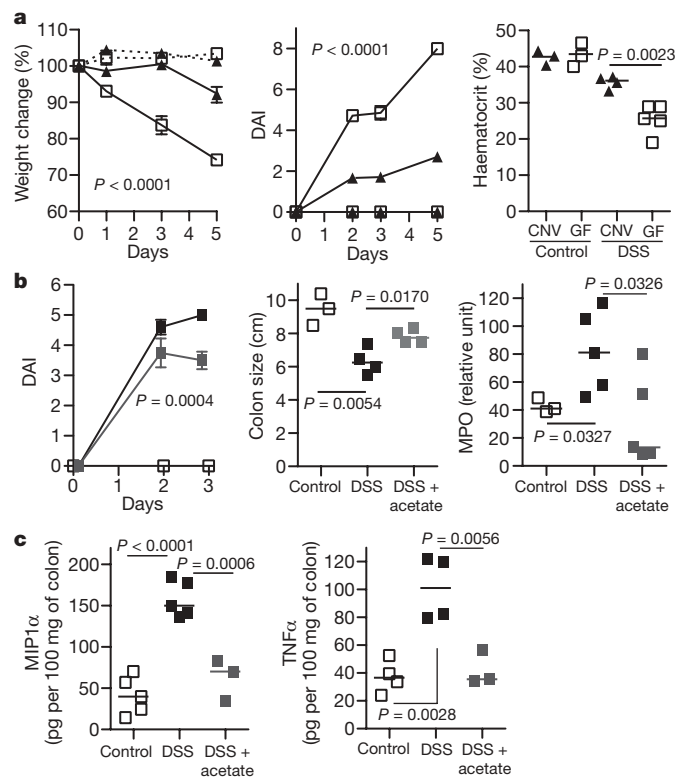


Figure 1 | Exacerbated colitis in germ-free mice is ameliorated by acetate.

a, Germ-free (open squares) and CNV (closed triangles) mice were given DSS colitis (4%, $n = 7$ (experimental groups)). Dashed lines, control mice; solid lines, DSS-treated mice. The percentage weight change (left), DAI (middle) and haematocrit (right) were measured. **b**, Germ-free mice were fed acetate (grey squares; 150 mM; $n = 3$) in the drinking water or water only (black squares; $n = 5$), 5 days before and during DSS administration. Control fed denotes no DSS (open squares). Daily activity score (left), colon length (middle) and colonic MPO (right) were determined. **c**, MIP1 α and TNF α levels in acetate-fed mice. Data are median \pm s.e.m., representative of two independent experiments.

¹Garvan Institute of Medical Research, 384 Victoria Street, Darlinghurst, New South Wales 2010, Australia. ²Cooperative Research Center for Asthma and Airways, Camperdown, New South Wales 2050, Australia. ³St Vincent's Clinical School, University of New South Wales, New South Wales 2010, Australia. ⁴Department of Biochemistry and Immunology, Instituto de Ciencias Biológicas, Universidade Federal de Minas Gerais, Belo Horizonte, Minas Gerais 31270-901, Brazil. ⁵Center for Computational and Integrative Biology and Gastrointestinal Unit, Massachusetts General Hospital and Harvard Medical School, 185 Cambridge Street, Boston, Massachusetts 02114, USA. ⁶Faculty of Medicine, Monash University, Wellington Road, Clayton, Victoria 3800, Australia. ⁷School of Veterinary Medicine, University of Pennsylvania, Philadelphia, Pennsylvania 19104, USA. ⁸Broad Institute of MIT and Harvard, Cambridge, Massachusetts 02142, USA.

(Fig. 1b), and decreased levels of $TNF\alpha$ and inflammatory MIP1 α (also known as CCL3) (Fig. 1c). SCFAs have a well-characterized anti-inflammatory effect, on both colonic epithelium and immune cells^{14–17}. Recently, SCFAs, particularly acetate (C2) and propionate (C3), have been found to bind and activate the G-protein-coupled receptor GPR43 (refs 10, 11). Using an extensive data set of human and mouse immune cell transcription profiles¹⁸ we found that transcripts for human *GPR43* and mouse *Gpr43* exhibited enhanced expression in neutrophils and eosinophils (Fig. 2a and Supplementary Fig. 2). Using nearest-neighbour

correlation analysis we found that *GPR43* gene expression was closely regulated with receptors important for innate immunity, such as Toll-like receptors (TLR2 and TLR4), formyl peptide receptors (FPR1 and FPR2), IL8RB (also known as CXCR2) and C5aR (Fig. 2a). We constructed protein interaction networks for genes co-regulated with GPR43, and, using a molecular complex detection and a graph-theory-based clustering (MCODE) algorithm¹⁹, we identified densely connected local sub-network clusters, revealing modules associated with apoptosis and innate immunity-related processes (Supplementary Fig. 3).

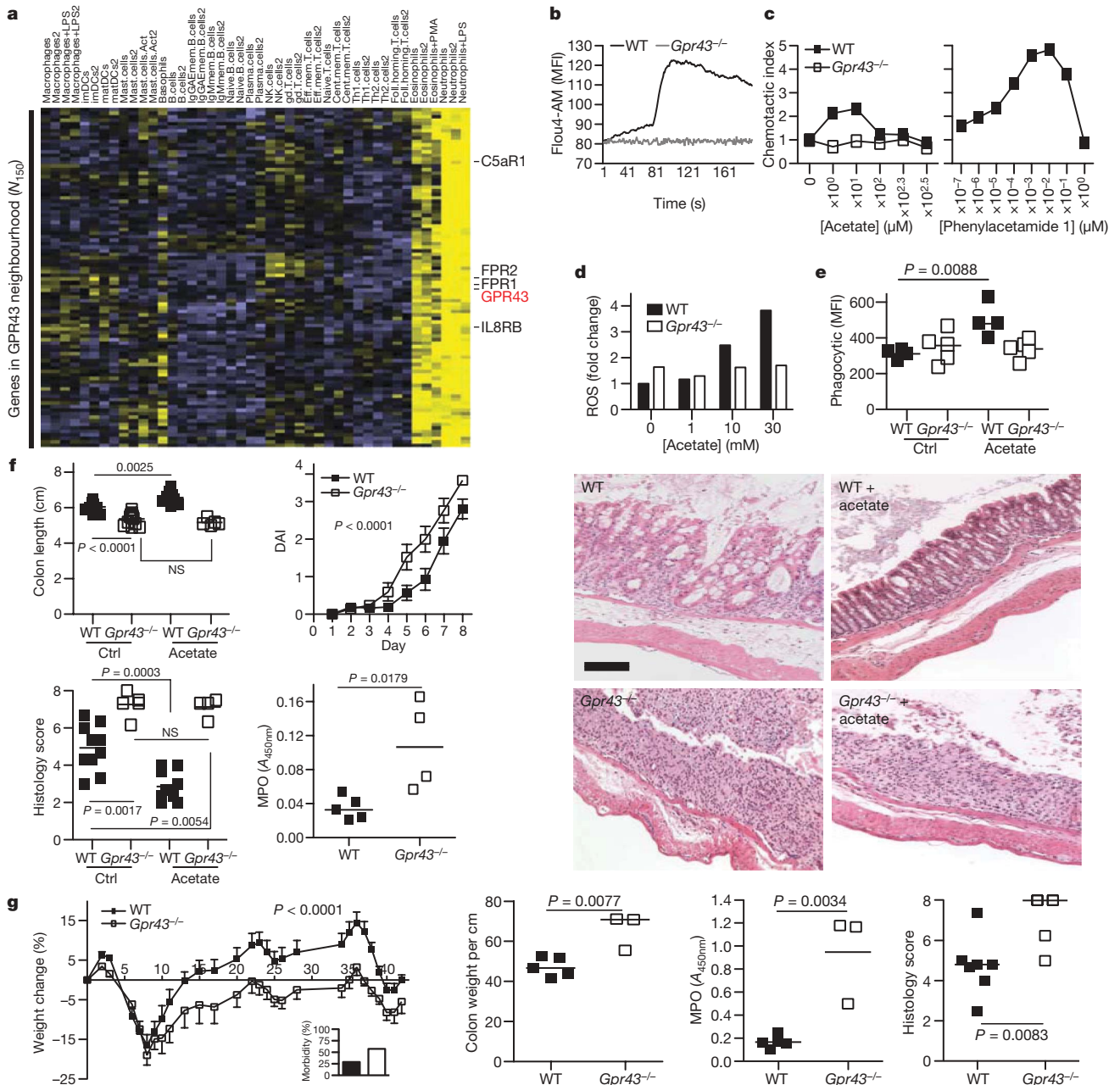


Figure 2 | GPR43 expression and role in inflammatory responses.

a, Immune expression signature of genes encoding cellular receptors across a large panel of leukocyte subsets. Clustering of receptor genes exhibiting enriched expression in neutrophils and eosinophils reveals GPR43, along with other receptors important for innate immunity and chemoattractant-induced responses. Correlation analysis across a wider set of genes in this immune panel identified a rank-ordered list of the top 150 genes (N_{150}) in the co-expression neighbourhood of GPR43. **b–e**, Comparison of wild-type (WT) and *Gpr43*^{-/-} bone marrow neutrophils with respect to acetate-induced Ca²⁺ flux (**b**; MFI, mean fluorescence intensity), chemotaxis (**c**, left panel), ROS production (**d**), and phagocytosis of fluorescently labelled

S. aureus (**e**). The right panel of **c** shows the GPR43 synthetic agonist phenylacetamide 1 in human neutrophil chemotaxis. **f**, DSS colitis (2.5% (w/v)) in wild-type and *Gpr43*^{-/-} mice, fed with acetate or control water (Ctrl). Shown are colon length, the DAI, histology score and colon MPO levels. NS, not significant. The far right panels show representative histological sections from wild-type or *Gpr43*^{-/-} mice as indicated (scale bar, 50 μ m). **g**, Chronic DSS-induced colitis ($n = 7$ per group, median \pm s.e.m.). The inset shows the percentage morbidity. Shown are the percentage change in weight, colon weight per cm of colon, colonic MPO, and histological score, for wild-type and *Gpr43*^{-/-} mice.

To demonstrate that GPR43 was the relevant receptor for SCFA effects on immune cells, we sourced *Gpr43*^{-/-} mice (Supplementary Fig. 4), and found that T- and B-cell numbers were normal, and their blood neutrophil numbers were in the normal range (not shown). Acetate induced a robust calcium flux in mouse neutrophils (as well as in human neutrophils and eosinophils, not shown), but not in neutrophils from *Gpr43*^{-/-} mice (Fig. 2b), indicating that GPR43 is the sole functional receptor for SCFAs on neutrophils. GPR43 has previously been reported to act as a chemoattractant receptor for acetate¹¹, and we found that neutrophils from wild-type, but not *Gpr43*^{-/-} mice, responded chemotactically to acetate, but only at very high concentrations (~100–1,000 μM), and with a relatively low chemotactic index (Fig. 2c). This may relate to the low affinity of GPR43 for SCFAs²⁰, the high concentrations of SCFAs normally present in tissues (0.1–10 mM in serum, and 200 mM in the colon)^{11,13}, and the need for chemoattractant receptors to sense a gradient. However, a recently reported synthetic agonist specific for human GPR43 with >100-fold potency over SCFAs²⁰ was much more robust in chemotaxis assays (Fig. 2c). In neutrophils from wild-type mice, but not *Gpr43*^{-/-} mice, SCFAs induced release of ROS and increased phagocytic activity (Fig. 2d, e) similar to activities reported for certain other chemoattractant receptors.

The characteristic expression pattern of GPR43 to cell types involved in innate immunity and inflammation, and the GPR43-dependent effects of SCFA neutrophil function suggested that GPR43 may be the relevant receptor on immune cells for the regulation of inflammatory responses by SCFAs. We induced colitis by adding DSS to the drinking water of *Gpr43*^{-/-} and wild-type littermate mice. In the acute phase (7 days), *Gpr43*^{-/-} mice showed a marked increase in their inflammatory response, compared to wild-type mice (Fig. 2f), including a reduced colon length, and an increased DAI, more severe inflammation by histological analysis and increased MPO activity in the colon, indicating increased neutrophil infiltration/activation (Fig. 2f). We next determined whether acetate protected against colitis in the acute DSS model, in a GPR43-dependent manner. Mice fed 200 mM acetate in their drinking water showed a substantial decrease in inflammation, as judged by longer colon length, a reduced DAI, reduced inflammatory infiltrate and less tissue damage, when compared to wild-type mice not fed acetate (Fig. 2f). Notably, this protection occurred by acetate binding to GPR43, because acetate had no beneficial effect in *Gpr43*^{-/-} mice (Fig. 2f).

In a chronic model of DSS-induced colitis, *Gpr43*^{-/-} mice showed greater morbidity (at day 8, Fig. 2g, inset), and a marked reduction in the ability to regain weight compared to wild-type littermates (Fig. 2g). By day 42, *Gpr43*^{-/-} mice showed reduced colon length, increased colon histology score, as well as increased MPO levels in the colon. In a T-cell-dependent model of colitis, the TNBS (trinitrobenzoic sulphonic acid)-induced model, *Gpr43*^{-/-} mice also had more severe disease with decreased colon length and increased colon histological scores (Supplementary Fig. 5). CD44⁺ IL17⁺ T cells in the mesenteric lymph nodes in this model were increased in *Gpr43*^{-/-} mice, as were transcripts for IL17A, IL6, IL1β, IFNγ and CCL2 in colon tissue (Supplementary Fig. 5).

GPR43 is also expressed on colonic epithelium, and SCFAs affect several functions of these cells including proliferation, and epithelial barrier function²¹ and butyrate is a major source of energy for colonocytes. We determined the contribution of immune and non-immune cells to the colitis phenotype we observed in *Gpr43*^{-/-} mice by using bone marrow chimeras (Supplementary Fig. 6). After 7 weeks of bone marrow reconstitution, colitis was induced by DSS in the drinking water. Wild-type mice reconstituted with *Gpr43*^{-/-} bone marrow showed a similar exacerbated inflammatory response in the colon, compared to *Gpr43*^{-/-} mice receiving *Gpr43*^{-/-} bone marrow, demonstrating that immune cells were largely responsible for the phenotype observed in *Gpr43*^{-/-} mice.

SCFA levels in the colon can be high, particularly after ingestion of large amounts of fibre, and SCFAs are rapidly absorbed and distribute systemically through the blood²². We therefore assessed peripheral inflammatory responses in *Gpr43*^{-/-} mice using the K/BxN serum-induced model of inflammatory arthritis and an ovalbumin (OVA)-induced model of allergic airway inflammation. In the inflammatory arthritis model *Gpr43*^{-/-} mice showed a slight delay in the onset of symptoms, but by day 11 inflammation in *Gpr43*^{-/-} mice was markedly more severe than in wild-type littermates, clinically and histologically, and did not resolve over the 28 days of study (Fig. 3a). *Gpr43*^{-/-} mice showed increased levels of MPO production by peripheral blood cells (Fig. 3a). Acetate in the drinking water 1 week before, and during, the induction of inflammatory arthritis reduced inflammation (Supplementary Fig. 7a). Germ-free mice given K/BxN serum also showed increased inflammation and a much slower resolution of inflammation when compared to CNV housed mice (Supplementary Fig. 7b). *Gpr43*^{-/-} mice also showed more severe inflammation compared with

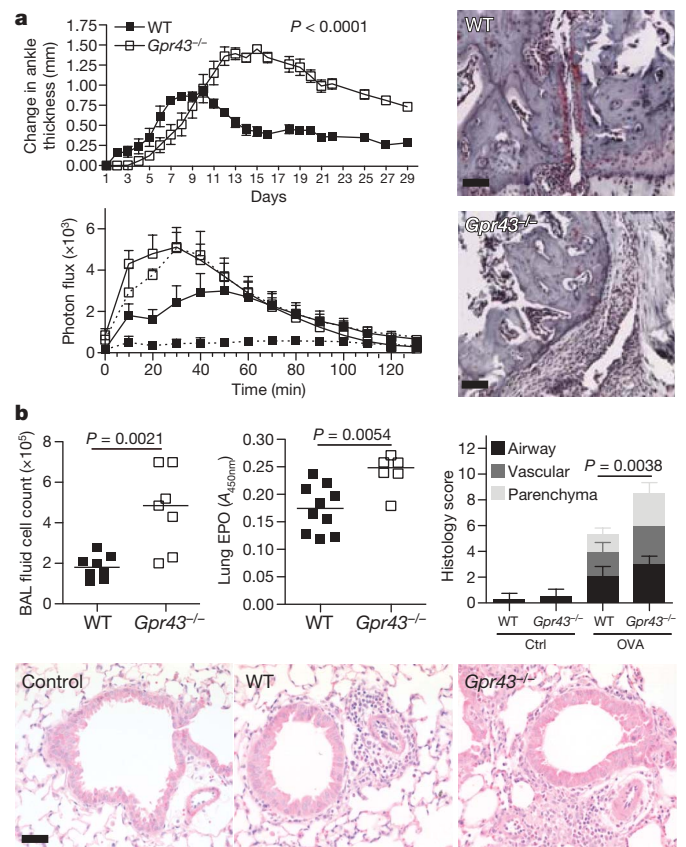


Figure 3 | Inflammatory arthritis and allergic airway disease and GPR43 deficiency. **a**, Inflammatory arthritis (K/BxN serum injection on day 0 and 2) in *Gpr43*^{-/-} mice ($n = 5$) versus wild-type littermates ($n \geq 3$). Scores shown are mean \pm s.e.m. for each time point, representative of three independent experiments. Wild-type mice are represented with closed squares, *Gpr43*^{-/-} mice with open squares, controls with dashed lines, and arthritic mice with solid lines. Change in ankle thickness (top) and measurement of MPO in the peripheral blood (bottom) showed that both naive and arthritic *Gpr43*^{-/-} mice had higher MPO production when stimulated with phorbol 12-myristate 13-acetate (PMA; bottom), indicating greater neutrophil activation ($P < 0.001$ *Gpr43*^{-/-} control compared to wild-type control, $P = 0.0019$ *Gpr43*^{-/-} compared to wild-type arthritic). Histological assessment at day 18 (right) (scale bars, 50 μm). **b**, OVA-induced allergic airway inflammation. BAL fluid cell counts (left), eosinophil peroxidase (EPO) activity in lung tissue (middle), and inflammation as scored by histology (right). The bottom panel shows representative haematoxylin-and-eosin-stained lung sections from wild-type and *Gpr43*^{-/-} mice, and control (no OVA) mice. Scale bar, 50 μm.

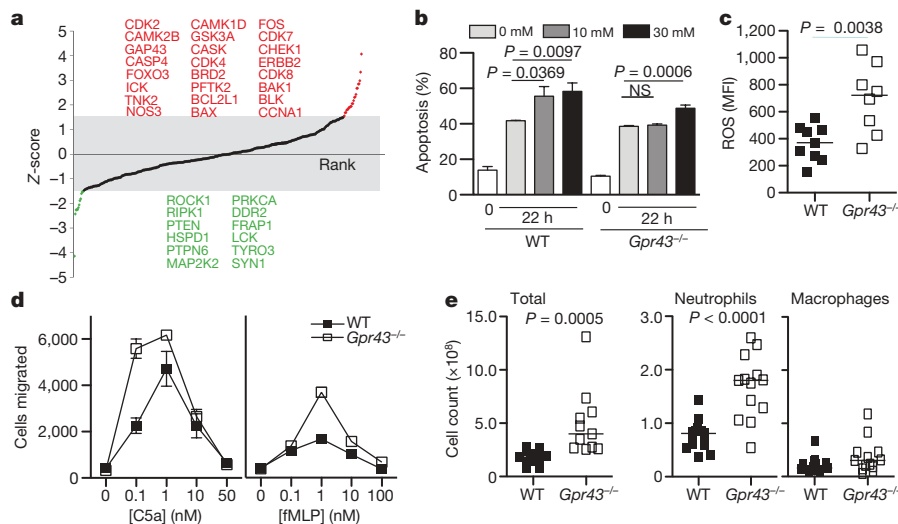


Figure 4 | GPR43 signalling and immune cell functions. **a**, Protein expression analysis using Kinex antibody microarrays. Z-score-transformed values reflecting positive or negative shifts in differential protein expression fold-changes after acetate treatment of neutrophils from wild-type mice compared to that from *Gpr43*^{-/-} mice. Proteins highlighted in red or green indicate those with Z-scores above +1.5 or below -1.5, respectively. **b**, Apoptosis in wild-type and *Gpr43*^{-/-} bone marrow cells, with or without

wild-type littermates in an acute allergic airway inflammation model, with increased numbers of cells in the broncho-alveolar lavage (BAL) fluid, as well as greater levels of eosinophil peroxidase and inflammatory cells in the lung tissue (Fig. 3b).

The cellular and molecular basis for GPR43–SCFA effects on inflammatory responses was studied using Kinex protein microarrays that interrogate more than 600 proteins and phosphoproteins. Because SCFAs also inhibit histone deacetylases and thereby affect cell transcription and functions²³, we made direct comparisons between wild-type and *Gpr43*^{-/-} neutrophils, to identify GPR43-related signalling pathways affected by SCFAs. Protein–protein interaction networks were constructed from the set of top-ranked proteins exhibiting greatest positive or negative differential shifts (Z -scores ≥ 1.5 and ≤ -1.5 ; Fig. 4a). We applied the MCODE clustering algorithm to identify highly connected local sub-networks, which revealed interesting modules such as the apoptosis-associated BAX–BAK1–BCL2L1 cluster and the PRKCA–PTPN6–LCK cluster (Supplementary Fig. 8a). Consistent with the changes in apoptosis-related signalling molecules, acetate induced apoptosis in neutrophils in a dose-dependent and a GPR43-dependent manner (Fig. 4b), except at very high concentrations (30 mM). There were also differences between wild-type and *Gpr43*^{-/-} neutrophils with respect to several other signalling pathways associated with inflammation, cell migration or apoptosis in mouse, and in human (Supplementary Figs 9 and 10). Granulocytes from *Gpr43*^{-/-} mouse blood showed an increase in levels of ROS (Fig. 4c) and MPO (Fig. 3a). Interestingly, macrophages from germ-free mice also show increased production of ROS²⁴. *Gpr43*^{-/-} neutrophils also showed increased chemotaxis to the *N*-formyl peptide f-Met-Leu-Phe (fMLP) and to the complement fragment C5a (Fig. 4d), compared to wild-type cells. Furthermore, heat-inactivated *Staphylococcus aureus* injected into the peritoneum of *Gpr43*^{-/-} mice yielded a greater recruitment of neutrophils after 1 h, compared to wild-type mice (Fig. 4e). Acetate stimulation of human neutrophils markedly reduced surface expression of pro-inflammatory receptors such as C5aR and CXCR2 (Supplementary Fig. 11), presumably through agonist-mediated receptor heterodimerization and internalisation.

Commensal bacteria and vertebrate immune systems form a symbiotic relationship and have co-evolved²⁵ such that proper immune development and function relies on colonisation of the gastrointestinal tract by commensal bacteria^{2,26}. SCFA–GPR43 signalling

acetate stimulation (apoptotic cells are annexin V and propidium iodide (PI) double positive). **c**, Chemotactic response to fMLP and C5a by wild-type and *Gpr43*^{-/-} bone marrow granulocytes. **d**, Recruitment of neutrophils and macrophages to the peritoneum in wild-type and *Gpr43*^{-/-} mice, injected with 1×10^6 heat-inactivated *S. aureus* particles. **e**, Reactive oxygen species production by peripheral blood granulocytes.

is one of the molecular pathways whereby commensal bacteria regulate immune and inflammatory responses. GPR43 resembles another anti-inflammatory chemoattractant receptor, ChemR23 (ref. 27), although this receptor binds endogenous rather than bacterially produced ligands. Any agents that affect gastrointestinal microbiota, and the production of SCFAs, might be expected to influence immune and inflammatory responses. It is possible that high levels of SCFAs such as acetate may, in addition to its direct effects on the GPR43 response, affect the biosynthesis of endogenous fatty acids, such as resolvins, that modulate leukocyte functions. Levels of SCFAs in the gastrointestinal tract vary significantly depending on the amount of non-digestible fibre in the diet, and also relate to the composition of the gut microbiota¹². For instance, the relative proportion of Bacteroidetes is decreased in obese people compared to lean people²⁸. Indeed an altered composition of the gut microbiota, brought on by western diet, or by use of antibiotics, has been suggested as a reason for the increased incidence of allergies and asthma in humans²⁹. SCFA–GPR43 interactions could represent a central mechanism to account for affects of diet, prebiotics and probiotics on immune responses, and may represent new avenues for understanding and potentially manipulating immune responses.

METHODS SUMMARY

RNA extraction, preparation, hybridization and expression analysis using U133A and B Affymetrix GeneChips (Gene Expression Omnibus (GEO) accession GSE3982) were performed as previously described, using an extensive collection of immune cell data sets¹⁸. Protein expression and phosphorylation were assessed using Kinex antibody microarrays (Kinexus Bioinformatics) (<http://www.kinexus.ca/services>). *Gpr43*^{-/-} mice on a C57Bl/6 background were obtained from Deltagen (<http://www.deltagen.com>). The K/BxN inflammatory arthritis model, the DSS and TNBS models of colitis, and the OVA allergic airway inflammation followed standard published procedures. Statistical analyses were conducted using a Student's two-way *t*-test, or two-way analysis of variance (ANOVA) using Graphpad Prism software.

Full Methods and any associated references are available in the online version of the paper at www.nature.com/nature.

Received 7 August; accepted 18 September 2009.

- Wen, L. *et al.* Innate immunity and intestinal microbiota in the development of Type 1 diabetes. *Nature* 455, 1109–1113 (2008).

2. Mazmanian, S. K., Round, J. L. & Kasper, D. L. A microbial symbiosis factor prevents intestinal inflammatory disease. *Nature* **453**, 620–625 (2008).
3. Frank, D. N. *et al.* Molecular-phylogenetic characterization of microbial community imbalances in human inflammatory bowel diseases. *Proc. Natl Acad. Sci. USA* **104**, 13780–13785 (2007).
4. Treem, W. R., Ahsan, N., Shoup, M. & Hyams, J. S. Fecal short-chain fatty acids in children with inflammatory bowel disease. *J. Pediatr. Gastroenterol. Nutr.* **18**, 159–164 (1994).
5. Harig, J. M., Soergel, K. H., Komorowski, R. A. & Wood, C. M. Treatment of diversion colitis with short-chain-fatty acid irrigation. *N. Engl. J. Med.* **320**, 23–28 (1989).
6. Kanauchi, O. *et al.* Treatment of ulcerative colitis by feeding with germinated barley foodstuff: first report of a multicenter open control trial. *J. Gastroenterol.* **37** (suppl. 14), 67–72 (2002).
7. Breuer, R. I. *et al.* Rectal irrigation with short-chain fatty acids for distal ulcerative colitis. Preliminary report. *Dig. Dis. Sci.* **36**, 185–187 (1991).
8. Scheppach, W. Treatment of distal ulcerative colitis with short-chain fatty acid enemas. A placebo-controlled trial. German-Austrian SCFA Study Group. *Dig. Dis. Sci.* **41**, 2254–2259 (1996).
9. Vernia, P. *et al.* Short-chain fatty acid topical treatment in distal ulcerative colitis. *Aliment. Pharmacol. Ther.* **9**, 309–313 (1995).
10. Brown, A. J. *et al.* The Orphan G protein-coupled receptors GPR41 and GPR43 are activated by propionate and other short chain carboxylic acids. *J. Biol. Chem.* **278**, 11312–11319 (2003).
11. Le Poul, E. *et al.* Functional characterization of human receptors for short chain fatty acids and their role in polymorphonuclear cell activation. *J. Biol. Chem.* **278**, 25481–25489 (2003).
12. Macfarlane, S. & Macfarlane, G. T. Regulation of short-chain fatty acid production. *Proc. Nutr. Soc.* **62**, 67–72 (2003).
13. Høverstad, T. & Midtvedt, T. Short-chain fatty acids in germfree mice and rats. *J. Nutr.* **116**, 1772–1776 (1986).
14. Tedelind, S., Westberg, F., Kjerrulf, M. & Vidal, A. Anti-inflammatory properties of the short-chain fatty acids acetate and propionate: a study with relevance to inflammatory bowel disease. *World J. Gastroenterol.* **13**, 2826–2832 (2007).
15. Cavaglieri, C. R. *et al.* Differential effects of short-chain fatty acids on proliferation and production of pro- and anti-inflammatory cytokines by cultured lymphocytes. *Life Sci.* **73**, 1683–1690 (2003).
16. Segain, J. P. *et al.* Butyrate inhibits inflammatory responses through NFκB inhibition: implications for Crohn's disease. *Gut* **47**, 397–403 (2000).
17. Lührs, H. *et al.* Butyrate-enhanced TNFα-induced apoptosis is associated with inhibition of NF-κB. *Anticancer Res.* **22**, 1561–1568 (2002).
18. Jeffrey, K. L. *et al.* Positive regulation of immune cell function and inflammatory responses by phosphatase PAC-1. *Nature Immunol.* **7**, 274–283 (2006).
19. Bader, G. D. & Hogue, C. W. An automated method for finding molecular complexes in large protein interaction networks. *BMC Bioinformatics* **4**, 2 (2003).
20. Lee, T. *et al.* Identification and functional characterization of allosteric agonists for the G protein-coupled receptor FFA2. *Mol. Pharmacol.* **74**, 1599–1609 (2008).
21. Suzuki, T., Yoshida, S. & Hara, H. Physiological concentrations of short-chain fatty acids immediately suppress colonic epithelial permeability. *Br. J. Nutr.* **100**, 297–305 (2008).
22. Pomare, E. W., Branch, W. J. & Cummings, J. H. Carbohydrate fermentation in the human colon and its relation to acetate concentrations in venous blood. *J. Clin. Invest.* **75**, 1448–1454 (1985).
23. Grunstein, M. Histone acetylation in chromatin structure and transcription. *Nature* **389**, 349–352 (1997).
24. Mørland, B. & Midtvedt, T. Phagocytosis, peritoneal influx, and enzyme activities in peritoneal macrophages from germfree, conventional, and ex-germfree mice. *Infect. Immun.* **44**, 750–752 (1984).
25. Ley, R. E. *et al.* Evolution of mammals and their gut microbes. *Science* **320**, 1647–1651 (2008).
26. Rakoff-Nahoum, S., Paglino, J., Eslami-Varzaneh, F., Edberg, S. & Medzhitov, R. Recognition of commensal microflora by toll-like receptors is required for intestinal homeostasis. *Cell* **118**, 229–241 (2004).
27. Serhan, C. N., Chiang, N. & Van Dyke, T. E. Resolving inflammation: dual anti-inflammatory and pro-resolution lipid mediators. *Nature Rev. Immunol.* **8**, 349–361 (2008).
28. Ley, R. E., Turnbaugh, P. J., Klein, S. & Gordon, J. I. Microbial ecology: human gut microbes associated with obesity. *Nature* **444**, 1022–1023 (2006).
29. Shreiner, A., Huffnagle, G. B. & Noverr, M. C. The "Microflora Hypothesis" of allergic disease. *Adv. Exp. Med. Biol.* **635**, 113–134 (2008).

Supplementary Information is linked to the online version of the paper at www.nature.com/nature.

Acknowledgements The authors thank P. Silvera and S. Tangye for supply of certain Genechip data sets, L. Tsai for help with heatmaps, and D. Kobuley, J. Nicoli and M. Abt for help in the germ-free animal facilities. K.M.M. and C.R.M. are supported by the Australian NHMRC, and the CRC for Asthma and Airways. A.N. is a recipient of a Fellowship award from the Crohn's and Colitis Foundation of America. F.S. and D.Y. are Cancer Institute NSW Fellows.

Author Contributions C.R.M. conceived and supervised the project, and K.M.M. performed the vast majority of the *in vitro* and *in vivo* experiments (other than those detailed below) and provided intellectual input to scientific direction and interpretations. A.T.V., M.M.T. and D.A. contributed to experiments with germ-free mice. F.M., M.S.R. and F.S. identified GPR43 as a receptor with an interesting transcript expression, and A.N. and R.J.X. were responsible for all of the subsequent bioinformatic analyses. H.C.S., D.Y. and J.K. provided general support for many of the experiments.

Author Information Reprints and permissions information is available at www.nature.com/reprints. Correspondence and requests for materials should be addressed to C.R.M. (charles.mackay@med.monash.edu.au).

METHODS

Microarray gene expression analysis. RNA extraction, preparation, hybridization and expression analysis using U133A and B Affymetrix GeneChips were performed as previously described, using an extensive immune cell data set³⁰. For analysis of immune cell data sets, MAS5-normalized data was filtered to remove probe sets identified as 'absent' (MAS5 algorithm) across all samples. The data was further filtered by setting a minimum threshold value >20 in at least one sample for each probeset and a maximum-minimum expression value >100. The data was then log- and Z-score-transformed. Pearson correlation coefficients were calculated for each pair of genes as well as for *GPR43*, and each gene represented on the array and k-means clustering performed³¹. Heatmaps were generated using TreeView³².

Kinex protein microarrays. Preparation of samples was done according to standard Kinexus recommendations (<http://www.kinexus.ca/services>). The normalized data from Kinexus was further filtered to remove data points with error ranges exceeding Kinexus's suggested threshold of 15% for adjacent duplicate spots. Positive or negative shifts in log expression fold-changes after SCFA treatment of *Gpr43*^{-/-} cell samples compared to that from wild-type samples were Z-score-transformed, identifying only top-scoring proteins with Z-scores above +1.5 or below -1.5.

Human protein interaction networks. Protein-protein interaction networks were constructed by iteratively connecting interacting proteins using curated data from the Human Protein Reference Database (HPRD)³³. The network uses graph theoretic representations which use abstract components (gene products) as nodes and relationships (interactions) between components as edges, implemented in the Perl programming language.

Neutrophil assays. Human neutrophils were isolated from the peripheral venous blood of healthy volunteers, using 1% dextran sedimentation for 30 min followed by centrifugation over 65% Percoll (Amersham Bioscience). Mouse neutrophils were isolated from hind leg femurs and separated by density centrifugation over Ficoll-Paque (Amersham Bioscience).

Reactive oxygen species were detected using H₂DCFDA (Sigma), as per manufacturer's directions. Twenty-five microlitres of 10 μM DCFDA was incubated with 25 μl whole blood for 20 min at 37 °C. Cells were then fixed, and red blood cells lysed. Cells were resuspended in FACS buffer.

Phagocytosis was assessed using fluorescently labelled Bioparticles, *Escherichia coli* K-12 strain or *S. aureus* (wood strain without protein A)-BODIPYFL conjugates (Molecular Probes). *In vitro*: 25 μl of whole blood was incubated with 3 × 10⁵ Bioparticles for 30 min, then analysed by flow cytometry. Chemotaxis was assessed using 3 μM Multiscreen-MIC 96-well plates (Millipore). Bone marrow neutrophils (3–5 × 10⁵) were in the top chamber, with chemoattractants in bottom chamber (fMLP, C5a, acetate, concentrations as shown in figures), cells and chemoattractants were in Chemotaxis buffer (50:50 RPMI and M199 + 2% BCS). Cell migration was assessed by flow cytometry as described previously³⁴. Apoptosis was assessed using Annexin V-FITC and propidium iodide as per manufacturer's instructions (Becton Dickinson).

Animals and models. All experimental procedures involving mice were carried out according to protocols approved by the relevant Animal Ethics Committees. *Gpr43*^{-/-} mice on a C57Bl/6 background were obtained from Deltagen. Housing and maintenance of germ-free mice followed previously described procedures^{35,36}. Germ-free mice were raised and housed germ free, as described previously³⁷.

Acute DSS colitis: mice were fed DSS in drinking water (percentage indicated in each figure) for 7 days and were monitored daily for stool score and visible bleeding. Stools were scored between 0 and 4, with 0 being normal up to 4 being diarrhoea, as described previously³⁸. At 7 days mice were killed and colons measured and assessed histologically using standard procedures. For bone marrow chimaeras, *Gpr43*^{-/-} (CD45.2) and congenic C57Bl/6 wild-type mice (CD45.1) were irradiated with 9 Gy then reconstituted with donor bone marrow (10⁷ cells) for 7 weeks. Reconstitution was checked by flow cytometry, using CD45 to determine bone marrow origin. For acetate-treatment experiments mice were fed acetate in the drinking water (concentration indicated in figure legends) for 5–7 days before DSS administration, and also in combination with DSS. MPO was detected as previously described³⁹. Colon

histology scoring was performed from adapted methods previously described. Damage was scored using the following system. Mucosal ulceration: 0, no injury; 1, focal injury; 2, multifocal injury; 3, diffuse ulceration/infiltration. Depth of injury: 0, no injury; 1, mucosal involvement only; 2, mucosal and submucosal involvement; 3, transmural involvement.

Chronic DSS colitis: Mice were fed DSS on days 0–6 (4%), 20–24 (2%) and 35–39 (4%), and killed on day 42. Mice were given normal drinking water in the rest periods. Disease was monitored as per the acute model.

TNBS-induced colitis: mice were sensitised by applying a mixture of acetone/olive oil (50:50) with TNBS (Sigma) (50:50, total) on shaved skin between shoulder blades. Seven days later, mice were challenged intra-rectally with 2.5 mg TNBS with 50% ethanol, 3.5 cm from the anal verge. Mice were fasted overnight before the intra-rectal challenge, and given 5% dextrose in the drinking water. Mice were killed 3 days after TNBS challenge.

For the K/BxN inflammatory arthritis model, 150 μl serum from K/BxN arthritic mice was used to induce experimental arthritis in recipient mice, and disease progression was monitored^{40,41}. The clinical score was calculated for each mouse by summing the scores for the four paws: 0, normal joint; 1, mild-to-moderate swelling of the ankle and/or one swollen digit; 2, swollen ankle or swelling in two or more digits; 3, severe swelling along all aspects of paw or all five digits swollen. For SCFA-feeding, sodium acetate was dissolved in drinking water at 200 mM (or as indicated) and fed to mice 1 week before colitis or arthritis induction, as well as during disease monitoring. Myeloperoxidase bioluminescence was detected in peripheral blood as described previously⁴².

Allergic airway disease was induced using OVA/alum as previously described⁴³ with modification. In brief, OVA/alum was injected interperitoneally on days 0 and 7, followed by intranasal challenge on days 12 to 15 and mice were killed on day 16. Eosinophil peroxidase was detected as previously described⁴⁴.

30. Liu, S. M. *et al.* Immune cell transcriptome datasets reveal novel leukocyte subset-specific genes and genes associated with allergic processes. *J. Allergy Clin. Immunol.* **118**, 496–503 (2006).
31. Eisen, M. B., Spellman, P. T., Brown, P. O. & Botstein, D. Cluster analysis and display of genome-wide expression patterns. *Proc. Natl Acad. Sci. USA* **95**, 14863–14868 (1998).
32. Saldanha, A. J. Java Treeview—extensible visualization of microarray data. *Bioinformatics* **20**, 3246–3248 (2004).
33. Mishra, G. R. *et al.* Human protein reference database—2006 update. *Nucleic Acids Res.* **34**, D411–D414 (2006).
34. Heath, H. *et al.* Chemokine receptor usage by human eosinophils. The importance of CCR3 demonstrated using an antagonistic monoclonal antibody. *J. Clin. Invest.* **99**, 178–184 (1997).
35. Souza, D. G. *et al.* The essential role of the intestinal microbiota in facilitating acute inflammatory responses. *J. Immunol.* **173**, 4137–4146 (2004).
36. Zaph, C. *et al.* Commensal-dependent expression of IL-25 regulates the IL-23–IL-17 axis in the intestine. *J. Exp. Med.* **205**, 2191–2198 (2008).
37. Souza, D. G. *et al.* The required role of endogenously produced lipoxin A4 and annexin-1 for the production of IL-10 and inflammatory hyporesponsiveness in mice. *J. Immunol.* **179**, 8533–8543 (2007).
38. Cooper, H. S., Murthy, S. N., Shah, R. S. & Sedergran, D. J. Clinicopathologic study of dextran sulfate sodium experimental murine colitis. *Lab. Invest.* **69**, 238–249 (1993).
39. Vieira, A. T. *et al.* Mechanisms of the anti-inflammatory effects of the natural secosteroids physalins in a model of intestinal ischaemia and reperfusion injury. *Br. J. Pharmacol.* **146**, 244–251 (2005).
40. Korganow, A. S. *et al.* From systemic T cell self-reactivity to organ-specific autoimmune disease via immunoglobulins. *Immunity* **10**, 451–461 (1999).
41. Lee, D. M. *et al.* Mast cells: a cellular link between autoantibodies and inflammatory arthritis. *Science* **297**, 1689–1692 (2002).
42. Gross, S. *et al.* Bioluminescence imaging of myeloperoxidase activity *in vivo*. *Nature Med.* **15**, 455–461 (2009).
43. Shum, B. O. *et al.* The adipocyte fatty acid-binding protein aP2 is required in allergic airway inflammation. *J. Clin. Invest.* **116**, 2183–2192 (2006).
44. Strath, M., Warren, D. J. & Sanderson, C. J. Detection of eosinophils using an eosinophil peroxidase assay. Its use as an assay for eosinophil differentiation factors. *J. Immunol. Methods* **83**, 209–215 (1985).